

Intratumoral T-cell composition predicts epcoritamab-based treatment efficacy in B-cell non-Hodgkin lymphomas

Lorenzo Falchi^{1,2*#}, Jahan Rahman^{3,4#}, Lauren Melendez³, Monifa Douglas¹, Walter Ramos Amador¹, Paul Hamlin^{1,2}, Anita Kumar^{1,2}, Daniela Hoehn⁵, Ya-Hui Lin³, Qi Gao⁶, Mikhail Roshal⁶, Mark D. Ewalt^{6,7}, Ahmet Dogan⁶, Benjamin Greenbaum⁴, Gilles A. Salles^{1,2}, Santosha A. Vardhana^{*1,2,3}

¹Department of Medicine, Lymphoma Service, Memorial Sloan Kettering Cancer Center, New York, NY

²Weill Cornell Medical College, New York, NY, USA

³Human Oncology and Pathogenesis Program, Memorial Sloan Kettering Cancer Center, New York, NY

⁴Department of Epidemiology and Biostatistics, Sloan-Kettering Institute, Memorial Sloan-Kettering Cancer Center, New York, NY

⁵Genmab, Princeton, NJ

⁶Hematopathology service, Department of Pathology and Laboratory Medicine, Memorial Sloan-Kettering Cancer Center, New York, NY

⁷Molecular Diagnostics Service, Department of Pathology and Laboratory Medicine, Memorial Sloan-Kettering Cancer Center, New York, NY

#Contributed equally

*Corresponding authors

Corresponding Authors:

- Lorenzo Falchi, Lymphoma Service, Department of Medicine, Memorial Sloan Kettering Cancer Center, 530 E 74th St, New York, NY 10021; email: falchil@mskcc.org; tel. +1646-608-3705;
- Santosha A. Vardhana; Lymphoma Service, Department of Medicine, Memorial Sloan Kettering Cancer Center, 417 E 68th St, New York, NY, 10065; vardhans@mskcc.org; tel. +1646-888-3285;

Lead contact: vardhans@mskcc.org

Summary

Leveraging endogenous tumor-resident T-cells for immunotherapy using bispecific antibodies (BsAb) targeting CD20 and CD3 has emerged as a promising therapeutic strategy for patients with B-cell non-Hodgkin lymphomas. However, features associated with treatment response or resistance are unknown. To this end, we analyzed data from patients treated with epcoritamab-containing regimens in the EPCORE NHL-2 trial (NCT04663347). We observed downregulation of CD20 expression on B-cells following treatment initiation both in progressing patients and in patients achieving durable complete responses (CR), suggesting that CD20 downregulation does not universally predict resistance to BsAb-based therapy. Single-cell immune profiling of tumor biopsies obtained following one cycle of therapy revealed substantial clonal expansion of cytotoxic CD4+ and CD8+ T-cells in patients achieving CR, and an expansion of follicular helper and regulatory CD4+ T-cells in patients whose disease progressed. These results identify distinct tumor-resident T-cell profiles associated with response or resistance to BsAb therapy.

Keywords (up to 10): Non-Hodgkin lymphoma; follicular lymphoma; diffuse large B-cell lymphoma; bispecific antibodies; epcoritamab; single-cell analysis; CD20; follicular helper T-cells

INTRODUCTION

Bispecific antibodies (BsAb) are the newest class of pharmaceuticals that promote T-cell dependent anti-tumor immunity, following the clinical development of antibodies targeting immune checkpoints such as PD-1 and CTLA-4 and of chimeric antigen receptor (CAR)-engineered T-cells. In patients with B-cell non-Hodgkin lymphoma (B-NHL), at least four BsAb co-targeting CD20 and CD3 (CD20xCD3), epcoritamab, glofitamab, mosunetuzumab, and odronextamab, have been developed with potent *in vitro* anti-tumor activity¹⁻⁵. These agents demonstrated frequent and durable responses in heavily pre-treated patients with relapsed or refractory (R/R) follicular lymphoma (FL) or diffuse large B-cell lymphoma (DLBCL), which led to regulatory approval in several countries⁶⁻⁹. This, in turn, promoted the rapid development of BsAb-based combinations with the objective of improving upon single-agent results, and early data appear promising¹⁰.

Despite this encouraging clinical activity, mechanisms of action of, and resistance to, BsAb are incompletely understood. We previously proposed three broad drivers of BsAb resistance, including antigen loss and either T-cell intrinsic or tumor- and T-cell-extrinsic inhibition of function¹⁰. CD20 loss, largely driven by somatic mutations resulting in either complete loss of expression or alternative splicing of the MS4A1 locus, does not appear to uniformly predict treatment resistance^{5,11-13}. Additionally, unlike CAR-T cells, BsAbs act by engaging the endogenous T-cells; therefore, their efficacy is likely to be impacted by both host immunologic features, including systemic and intratumoral T-cell composition, and BsAb characteristics, including capacity for T-cell recruitment and activation. To date, immune cell analyses conducted in patients

receiving BsAb therapy have not successfully distinguished patients with durable responses from those who experience disease progression¹⁴⁻¹⁶. In the present study, we analyzed primary on-treatment lymph node specimens obtained from patients with newly diagnosed or R/R B-NHL receiving epcoritamab-based combinations. We identified intratumoral B- and T-cell patterns associated with response and resistance to therapy.

RESULTS

Durable remission to BsAb-based therapy occurs despite CD20 downregulation

Biopsy material was available from 22 patients enrolled in the EPCORE NHL-2 trial (NCT04663347), including 9 patients with DLBCL (7 newly diagnosed and 2 with relapsed/refractory (R/R) disease) and 13 with FL (3 newly diagnosed and 10 with R/R disease) (**Fig. 1A**). Clinical characteristics of the patients are listed in **Table 1**. All patients with newly diagnosed DLBCL and FL achieved deep and durable complete responses (CR). Two patients with R/R DLBCL achieved a partial response (PR) followed by disease progression (PD). Nine out of 10 patients with R/R FL achieved a CR, with only one patient experiencing subsequent progression (PD), and one patient did not achieve a response.

To examine the effects of epcoritamab-based therapies on intratumoral immunophenotypic changes in B and T cells, we analyzed archival tissue available obtained from 15 patients prior to initiation of treatment with epcoritamab, on-treatment samples obtained within 4 weeks of treatment initiation (N=10 patients), and disease progression biopsies (N=3 patients). Additionally, we analyzed multiparametric flow

cytometry data from 15 pre-treatment, 5 on-treatment, and 1 progression biopsies (**Supplementary Table 1**). Lastly, we performed combined single-cell RNA and T-cell receptor (TCR) sequencing using the 10x Genomics Single Cell Immune Profiling Platform on 10 on-treatment samples for which single-cell dissociated and cryopreserved samples were available.

We first asked whether B-cell features were associated with response or resistance to BsAb-based therapies. We focused our analysis on FL patients, from whom most samples were obtained (10 pre-treatment, 5 on-treatment). CD20 expression was present on B-cells from all pre-treatment FL samples, as measured by both immunohistochemistry (IHC) (L26, which recognizes an intracellular epitope on CD20¹⁷) (**Supplementary Table 2**) and by flow cytometry (FC) (2H7, which recognizes an extracellular CD20 epitope¹⁸) (**Supplementary Table 3**). CD20 expression was retained in all pre-treatment samples with a characteristic membrane distribution, with no significant difference in expression of either CD20 or other B-cell markers between patients who did or did not achieve a durable CR (**Fig. 1B**). Immunohistochemical analysis of on-treatment and progression biopsies was notable for diminished or absent surface expression of CD20 in all examined cases (**Supplementary Table 4**). This could not be explained by epitope masking by either epcoritamab or rituximab, as the L26 antibody for IHC binds an intracellular CD20 epitope while epcoritamab or rituximab bind the extracellular region of CD20. In patients with PD (patients 16 and 20), abundant B-cells (defined by PAX-5 expression) lacking CD20 expression were clearly identified (**Fig. 1B**). In some patients achieving durable CRs (patient 11), loss of CD20

expression was due to a lack of viable B-cells present at the time of biopsy. However, in two patients (patients 10 and 16), both of whom achieved durable CRs, decreased surface CD20 expression despite clear residual PAX5+ cells were observed; in one case (patient 15) total CD20 levels were decreased while in one case (patient 10), CD20 was primarily cytoplasmic (**Supplementary Fig. 1A**). We confirmed loss of surface CD20 expression across on-treatment biopsies from FL patients using flow cytometry, although the activity of the 2H7 clone utilized in this assay may be impacted by rituximab (**Supplementary Fig. 1B**).

We next asked whether the mechanism of CD20 downmodulation might impact the therapeutic efficacy of BsAb-based therapy. Interestingly, while patient 20, whose best response was PD, expressed substantially lower transcript levels of *MS4A1* (the gene encoding CD20) compared with patients 10, 11, and 19, who achieved durable CR, no difference in CD20 protein expression was observed, suggesting post-transcriptional downregulation of CD20 expression in complete responders (**Supplementary Fig. 1C**). While alternative splicing of the *MS4A1* 5' untranslated region (UTR) has been reported as a post-transcriptional mechanism of CD20 loss and resistance to CD20-directed therapies¹¹, we did not observe accumulation of any annotated *MS4A1* splice variants (**Supplementary Fig. 1D**). Rather, analysis of differentially expressed genes between patients achieving a CR or PD as best response demonstrated an upregulation of several gene sets related to ribosomal biogenesis and RNA stability, suggesting that CD20 loss in patients achieving a CR may be regulated post-transcriptionally (**Fig 1C**). Consistent with this hypothesis, we observed a buildup of *MS4A1* reads in the 5' UTR

and first 2 coding exons of patients achieving a CR, suggesting that these transcripts might be either truncated or partially degraded (**Supplementary Fig. 1D**). Differential gene expression analysis of B-cells from patients achieving either CR or PD revealed that B-cells from the former were enriched for genes associated with interferon-gamma (IFN- γ) signaling and antigen processing and presentation, including MHC-II genes (*HLA-DQA2*, *HLA-DQB2*) and IFN- γ -responsive transcription factors (*STAT1*, *IRF1*) (**Fig. 1D**). In contrast, patient 20, who achieved PD as best response, expressed high levels of *MAP2K6*, which activates the p38 MAP kinase pathway and has been shown to accelerate B-cell proliferation and predict treatment failure in patients with B-cell lymphoma and which, more broadly, is associated with resistance to immunotherapy across cancer subtypes¹⁹⁻²².

The majority of DLBCL research samples were obtained from newly diagnosed patients receiving epcoritamab with R-CHOP (**Supplementary Table 1**). In these patients, CD20 analysis was confounded by substantial tissue necrosis and minimal residual PAX5+ B-cells, with CD20 expression restricted to grossly necrotic cells (**Supplementary Fig. 1E**). Interestingly, CD20 expression was strongly retained in the on-treatment sample from patient 8, who had R/R DLBCL treated with epcoritamab, gemcitabine and oxaliplatin. Both patients 8 and 9 exhibited complete loss of CD20 expression at the time of disease progression (**Supplementary Fig. 1E**).

Distinct intratumoral T-cell composition and function in BsAb responders

Next, we asked whether the intratumoral T-cell composition, either prior to, or following treatment with epcoritamab, was associated with response to therapy. Compared with patients who remained progression-free, pre-treatment samples from the 2 patients who experienced PD (one of whom had previously achieved CR) had substantially fewer CD8⁺ T-cells and a higher CD4:CD8 T-cell ratio (**Fig. 2A**). This difference persisted following treatment, suggesting that an intratumoral CD8⁺ T-cell bias may enable durable remissions after epcoritamab-based therapies.

To determine whether response to epcoritamab-based therapies was associated with quantitative or qualitative differences in intratumoral T-cell abundance or phenotype, we analyzed single-cell (sc) immune profiling data from on-treatment biopsies collected from 7 patients (2 with newly diagnosed FL, 3 with R/R FL, and 2 with R/R DLBCL). Four achieved a CR, 2 a PR and one had PD as their best response. After quality control filtering, we analyzed a total of 14,278 cells from these 7 patients (**Fig. 2B**). Seurat-based clustering of CD4⁺ and CD8⁺ T-cells identified known lymph node-resident phenotypes (**Fig. 2C**) including naïve CD4⁺ and CD8⁺ T-cells (expressing *IL7R*, *SELL*, *CCR7*), cytotoxic CD4⁺ T-cells (*GZMK*, *PRF1*, *NKG7*), follicular helper CD4⁺ T-cells (Tfh) (*CXCL13*, *TOX2*, *PDCD1*), regulatory T-cells (Treg) (*FoxP3*, *IL2RA*, *TNFRSF1B*), cytotoxic CD8⁺ T-cells (*S100A4*, *CXCR6*, *PRF1*), effector/memory CD8⁺ T-cells (*IL7R*, *SELL*, *S100A4*, *CX3CR1*), and exhausted CD8⁺ T-cells (*PDCD1*, *TOX*, *CXCL13*) (**Supplementary Fig. 2A-B**). Combined scRNA-sequencing (seq) and scTCR-seq revealed cell state-specific clonal expansion in both the CD4⁺ and CD8⁺ T-cell compartments (**Fig. 2D-E**). In patients achieving a CR, the majority of clonally

expanded T-cells in both the CD4+ and CD8+ T-cell compartments exhibited a cytotoxic phenotype, with expression of *CST7*, *CCL4*, and *NKG7* (**Fig. 2D-F and Supplementary Fig. 2C-D**). In contrast, the patient with PD as best response showed substantial expansion of CD4+ Tfh and Treg subsets with almost no CD8+ T-cell expansion. Patients achieving a PR exhibited an intermediate phenotype with less expansion of cytotoxic T-cells compared to CR patients and clonal expansion of CD8+ T-cells with an exhausted phenotype. Analysis of clonal expansion across patients and cell states revealed that patients achieving a CR exhibited a polyclonal, cytotoxic T-cell response, with high numbers of expanded cytotoxic CD4+ and CD8+ T-cell clones but relatively few medium (5-20) or large (21+) clones (**Fig. 2E-F**). Patients achieving a PR showed a more clonal CD4+ and CD8+ T-cell response, with high frequencies of large CD4+ T-cell clones with a memory, Treg, or Tfh phenotype and CD8+ T-cell clones with an exhausted phenotype. Finally, patients with PD had almost no expanded CD8+ T-cell clones but showed marked expansion of Tfh.

These results indicated that intratumoral T-cell composition can impact therapeutic response. To functionally confirm these findings, we co-cultured effector CD8+, Tregs, or Tfh^{23,24} with luciferase-expressing RAJI B-cells²⁵ in the presence of epcoritamab (**Fig. 3A and Supplementary Fig. 3A**). Epcoritamab induced substantial killing of RAJI cells when co-cultured with CD8+ T-cells; however, both CD4+ Tregs and CD4+ Tfh cells showed substantially reduced killing of malignant B-cells in response to Epcoritamab (**Fig. 3B**).

DISCUSSION

Bispecific antibodies represent a novel, highly effective therapeutic strategy in patients with B-cell non-Hodgkin lymphoma. These off-the-shelf drugs overcome some of the limitations of CAR-T cell therapy, including the requirement for lymphodepleting chemotherapy, prolonged time to infusion, and limited access to accredited cellular therapeutics departments. Epcoritamab is a potent CD20xCD3 BsAb that produced highly encouraging single-agent clinical results^{8,9} and was approved by several regulatory agencies worldwide for the treatment of adults with R/R LBCL after ≥ 2 lines of systemic therapy²⁶. Understanding determinants of response and resistance is, therefore, crucial for the continued development of this agent (and CD20xCD3 BsAbs as a class), particularly as the intratumoral cell composition and phenotype are known to influence lymphoma development and progression²⁷. To our knowledge, this represents the first characterization of the intratumoral immune response to epcoritamab-based treatments. Our results identify clonal expansion of T-cells with a cytotoxic phenotype in patients with durable response to therapy. We also identify, for the first time in primary samples from treated patients, *in situ* depletion of CD8+ T-cells and clonal expansion of CD4+ Treg or Tfh cells as markers of BsAb treatment failure. Historically, the prognostic and predictive role of different T-cell subsets in the lymphoma microenvironment following immunotherapies like PD-1/PD-L1 blockers or CAR-T cells, or BsAbs, has been difficult to dissect with IHC or flow cytometry, which lack adequate resolution. Single-cell RNAseq data combined with bioinformatic deconvolution in clinically annotated samples allowed us to begin to explore these potentially critical changes. Whether these specific to FL or more generalizable requires

further analysis of patient samples across B-NHL subtypes. Additionally, given the well-established role of Tfh cells in supporting lymphoma survival and growth²⁸⁻³¹, whether Tfh persistence or proliferation following BsAb therapy might enable lymphoma progression is an intriguing topic for future study. Regardless, our results suggest that strategies to limit engagement of non-cytotoxic CD4+ T-cells by BsAb may enhance response to treatment.

Our findings also indicate that, particularly in FL samples, decreased or absent CD20 protein expression as measured using standard clinical testing protocols may not uniformly predict resistance to CD20xCD3 BsAb as most patients achieved a durable CR, including at least 2 patients with CD20-negative B-cells after treatment. Nonetheless, understanding the mechanism of CD20 downregulation may be of particular importance in predicting treatment failure. Our finding of CD20 downregulation without loss of transcript expression is consistent with post-transcriptional regulation of CD20 surface expression. This raises the possibility that preventing CD20 internalization could enhance BsAb therapy, although we cannot exclude that low-level surface expression of CD20 in tumors with retained *MS4A1* transcript expression is sufficient to maintain BsAb efficacy. It is also conceivable that pre-existing CD20-negative clones expanded following treatment, although this appears less likely given the pervasive CD20 downregulation seen at the time of on-treatment biopsies. Finally, our observation that B-cells from patients achieving a durable CR upregulated genes associated with antigen presentation, in combination with the diverse and polyclonal cytotoxic T-cell response, suggests that IFN-driven antigen spreading

may contribute to durable BsAb-mediated anti-tumor immunity, though the functional importance of IFN- γ signaling and MHC-II upregulation on malignant B-cells remains undetermined.

The interpretation of our results is limited by the small sample size, the fact that additional agents were administered with epcoritamab, and the lack of systematic paired pre-treatment and on-treatment tumor biopsies obtained as part of this study. Nevertheless, our data clearly delineate distinct T-cell profiles in patients who achieved durable CR and those who did not and offer insights into possible strategies to overcome resistance to BsAb-based therapy.

ACKNOWLEDGEMENTS/ FUNDING: This work was supported by a Steven Greenberg Lymphoma Grant and a Priority Research Grant from the Lymphoma Research Foundation (S.A.V.), as well as MSKCC's Core Grant P30 CA008748. We thank Dr. Andrew Steele for his insightful input.

Author contributions: L.F. and G.S. designed and led the clinical trial with support from M.D., W.R.A., D.H., and A.S. L.F., P.H., and A.K and G.S. enrolled patients on the study. M.D.E. analyzed immunohistochemistry data. Q.G. and M.R. performed clinical flow cytometry experiments. J.R. and L.M. performed single-cell transcriptomic analysis with supervision by B.G. Y-H.L. performed *in vitro* assays with supervision by S.A.V. L.F., J.R., and S.A.V. authored the manuscript. All co-authors edited the manuscript and approved it in its final version.

Declaration of interests: L.F. Has received research funding from Genmab A/S, AbbVie, Inc., F. Hoffmann-La Roche AG, Genentech Inc., Innate Pharma S.A.; has provided consulting services for Genmab A/S, AbbVie, Inc., F. Hoffmann-La Roche AG, Genentech, Inc., Evolveimmune Therapeutics, Inc., Sanofi, S.A.; has served as an advisor for AbbVie, Inc., Seagen, Inc., Ipsen Biopharmaceuticals, Inc., ADC therapeutics S.A.; and has received travel reimbursement from Genmab A/S, AbbVie, Inc. S.A.V. previously served as an advisor for Immunai, has provided consulting services for ADT Therapeutics and Koch Disruptive Technologies, and has received funding from BMS. G.S. has received financial compensation for consulting services in the last 12 months from: Abbvie, Atb Therapeutics, Beigene, BMS, Genentech/Roche, Genmab, Janssen, Innate Pharma, Incyte, Ipsen, Kite/Gilead, Merck, Modex, Molecular Partners, Novartis, Nurix, Orna Therapeutics, and Treeline. He is a shareholder of Owkin. He has received research support from Abbvie, Genentech, Genmab, Janssen, Ipsen, and Nurix, which his institution managed.

Figure 1. Intratumoral phenotypic alterations in patients receiving epcoritamab-based therapies for B-NHL. (a) Schematic and outcomes of patients treated in NCT04663347. (b) Immunohistochemistry of lymph node biopsies obtained from patients with FL at the timepoints indicated. (c) Dot plot depicting enrichment of MSigDB genesets in B-cell scRNA-seq transcriptomes from patients achieving a CR vs. PD as best response. (d) Differentially expressed genes in B-cells between patients who achieved a CR (right) vs. PD (left) as best response. P values calculated using Student's t-test adjusted for multiple comparisons (d). FL, follicular lymphoma; DLBCL, diffuse large B-cell lymphoma; ND, newly diagnosed; RR, relapsed/refractory; CR, complete response; PD, progression of disease; H&E, hematoxylin and eosin; Epcor, epcoritamab; RCHOP, Rituximab, cyclophosphamide, vincristine, prednisone; GemOx, gemcitabine and oxaliplatin; Len, lenalidomide.

Figure 2. Single-cell immune profiling reveals distinct T-cell states associated with response or resistance to epcoritamab-based therapies. (a) abundance and proportions of CD4⁺ and CD8⁺ T-cells in lymph node biopsies assessed by flow cytometry. (b) UMAP of CD45⁺ T-cells from on-treatment biopsies, colored by coarse cell type. (c) UMAP of CD4⁺ (above) and CD8⁺ (below) T-cells, colored by phenotypic cluster. (d) Clonal abundance of CD4⁺ (above) and CD8⁺ (below) T-cells as measured by scTCR-seq, stratified by best response and projected in UMAP space. (e,f) Stacked bar plots showing either fraction of total expanded clones (>1 cell with the same TCR CDR3 sequence) derived from each phenotypic cluster depicted in (c), stratified by best

response (left), or clonal abundance, stratified by phenotypic cluster (right), for either CD4+ (e) or CD8+ (f) T-cells. P values calculated using Student's t-test (a).

Figure 3. Decreased bispecific antibody-dependent killing by CD4+ T-cell subsets. (a) Schematic for epcoritamab-dependent B-cell killing assay. (b) Fractional killing of RAJI B-cells by epcoritamab in the setting of co-culture with distinct T-cell subsets, measured by luciferase activity relative to culture with no T-cells.

Table 1. Clinical characteristics of patients treated on NCT #04663347.

Patient N.	Histology	Setting	Prior therapies	Best response	Last follow-up		
					Treatment	Response	Status
1	DLBCL, non-GCB	ND		CR	Completed	CR	A
2	DLBCL, non-GCB	ND		CR	Completed	CR	A
3	DLBCL (tFL), non-GCB	ND		CR	Completed	CR	A
4	DLBCL, non-GCB	ND		CR	Completed	CR	A
5	DLBCL, GCB	ND		CR	Completed	CR	A
6	DLBCL (tFL), GCB	ND		CR	Completed	CR	A
7	DLBCL	ND		CR	Completed	CR	A
8	DLBCL	RR	R-EPOCH; R-ICE; CAR-T	PR	Completed	PD	D
9	DLBCL, non-GCB	RR	R-CHOP/R-ICE; R-DHAX; CAR-T	PR	Completed	PD	D
10	FL, G1-2	ND		CR	Completed	CR	A
11	FL, G1-2	ND		CR	Completed	CR	A
12	FL, G3A	ND		CR	Ongoing	CR	A
13	FL, G1-2	RR	R-CHOP	CR	Completed	CR	A
14	FL, G1-2	RR	R-CHOP	CR	Ongoing	CR	A
15	FL, G1-2	RR	R-CHOP; R-len	CR	Ongoing	CR	A
16	FL, G1-2	RR	BR	CR	Completed	PD	A
17	FL, G3A	RR	R-CHOP	CR	Completed	CR	A
18	FL, G3A	RR	O-CVP; O-CEOP; RT	CR	Completed	CR	A
19	FL, G1-2 (prior DLBCL)	RR	R-CHP-polatuzumab (for DLBCL)	CR	Completed	CR	A
20	FL, G1-2 (prior DLBCL)	RR	R-EPOCH, R-GemOx, CAR-T, R-DHAX, O-len, other*	PD	Completed	PD	D
21	FL, G1-2	RR	O-CHOP	CR	Ongoing	CR	A
22	FL, G1-2	RR	O-CHOP, BR-HDT-ASCS	CR	Ongoing	CR	A

Study arms: 1, epcor-R-CHOP; 5, epcor-GemOx; 6 adn 2b, epcor_R-len. * pembrolizumab-entinostat, zanubrutinib-zandelisib both as part of a clinical trial. Abbreviations: DLBCL, diffuse large B-cell lymphoma; GCB, germinal center B; (t)FL, (transformed) follicular lymphoma; G, grade; ND, newly diagnosed; RR, relapsed or refractory; R, rituximab; EPOCH, etoposide, prednisone, vincristine, cyclophosphamide, doxorubicin; CAR-T, chimeric antigen receptor cell therapy; CHOP, rituximab, cyclophosphamide, doxorubicin, vincristine, prednisone; len, lenalidomide DHAX, dexamethasone, cytarabine, oxaliplatin, B, bendamustine; CVP, cyclophosphamide, vincristine, prednisone; GemOx, gemcitabine, oxaliplatin; HDT-ASCS, high-dose therapy adn autologous stem cell support; epcor, epcoritamab; CR, complete response; PR, partial response; PD, progressive disease; A, alive, D, dead.

REFERENCES

1. Engelberts, P.J., *et al.* DuoBody-CD3xCD20 induces potent T-cell-mediated killing of malignant B cells in preclinical models and provides opportunities for subcutaneous dosing. *EBioMedicine* **52**, 102625 (2020).
2. Frances, N., *et al.* Novel in Vivo and in Vitro Pharmacokinetic/Pharmacodynamic-Based Human Starting Dose Selection for Glofitamab. *J Pharm Sci* **111**, 1208-1218 (2022).
3. Sun, L.L., *et al.* Anti-CD20/CD3 T cell-dependent bispecific antibody for the treatment of B cell malignancies. *Sci Transl Med* **7**, 287ra270 (2015).
4. Bacac, M., *et al.* CD20-TCB with Obinutuzumab Pretreatment as Next-Generation Treatment of Hematologic Malignancies. *Clin Cancer Res* **24**, 4785-4797 (2018).
5. Brouwer-Visser, J., *et al.* Molecular assessment of intratumoral immune cell subsets and potential mechanisms of resistance to odronextamab, a CD20xCD3 bispecific antibody, in patients with relapsed/refractory B-cell non-Hodgkin lymphoma. *J Immunother Cancer* **12**(2024).
6. Budde, L.E., *et al.* Safety and efficacy of mosunetuzumab, a bispecific antibody, in patients with relapsed or refractory follicular lymphoma: a single-arm, multicentre, phase 2 study. *Lancet Oncol* **23**, 1055-1065 (2022).
7. Dickinson, M.J., *et al.* Glofitamab for Relapsed or Refractory Diffuse Large B-Cell Lymphoma. *N Engl J Med* **387**, 2220-2231 (2022).

8. Izutsu, K., *et al.* Subcutaneous epcoritamab monotherapy in Japanese adults with relapsed/refractory diffuse large B-cell lymphoma. *Cancer Sci* **114**, 4643-4653 (2023).
9. Thieblemont, C., *et al.* Epcoritamab, a Novel, Subcutaneous CD3xCD20 Bispecific T-Cell-Engaging Antibody, in Relapsed or Refractory Large B-Cell Lymphoma: Dose Expansion in a Phase I/II Trial. *J Clin Oncol* **41**, 2238-2247 (2023).
10. Falchi, L., Vardhana, S.A. & Salles, G.A. Bispecific antibodies for the treatment of B-cell lymphoma: promises, unknowns, and opportunities. *Blood* **141**, 467-480 (2023).
11. Ang, Z., *et al.* Alternative splicing of its 5'-UTR limits CD20 mRNA translation and enables resistance to CD20-directed immunotherapies. *Blood* **142**, 1724-1739 (2023).
12. Duell, J., *et al.* Sequential antigen loss and branching evolution in lymphoma after CD19- and CD20-targeted T-cell-redirecting therapy. *Blood* **143**, 685-696 (2024).
13. Schuster, S.J., *et al.* Loss of CD20 expression as a mechanism of resistance to mosunetuzumab in relapsed/refractory B-cell lymphomas. *Blood* **143**, 822-832 (2024).
14. Budde, L.E., *et al.* Single-Agent Mosunetuzumab Shows Durable Complete Responses in Patients With Relapsed or Refractory B-Cell Lymphomas: Phase I Dose-Escalation Study. *J Clin Oncol* **40**, 481-491 (2022).

15. Hutchings, M., *et al.* Glofitamab, a Novel, Bivalent CD20-Targeting T-Cell-Engaging Bispecific Antibody, Induces Durable Complete Remissions in Relapsed or Refractory B-Cell Lymphoma: A Phase I Trial. *J Clin Oncol* **39**, 1959-1970 (2021).
16. Hutchings, M., *et al.* Dose escalation of subcutaneous epcoritamab in patients with relapsed or refractory B-cell non-Hodgkin lymphoma: an open-label, phase 1/2 study. *Lancet* **398**, 1157-1169 (2021).
17. Mason, D.Y., Comans-Bitter, W.M., Cordell, J.L., Verhoeven, M.A. & van Dongen, J.J. Antibody L26 recognizes an intracellular epitope on the B-cell-associated CD20 antigen. *Am J Pathol* **136**, 1215-1222 (1990).
18. Klein, C., *et al.* Epitope interactions of monoclonal antibodies targeting CD20 and their relationship to functional properties. *MAbs* **5**, 22-33 (2013).
19. Craxton, A., *et al.* p38 MAPK is required for CD40-induced gene expression and proliferation in B lymphocytes. *J Immunol* **161**, 3225-3236 (1998).
20. Khiem, D., Cyster, J.G., Schwarz, J.J. & Black, B.L. A p38 MAPK-MEF2C pathway regulates B-cell proliferation. *Proc Natl Acad Sci U S A* **105**, 17067-17072 (2008).
21. Luke, J.J., *et al.* Tumor cell p38 inhibition to overcome immunotherapy resistance. *Res Sq* (2023).
22. Vega, G.G., *et al.* P38 MAPK expression and activation predicts failure of response to CHOP in patients with Diffuse Large B-Cell Lymphoma. *BMC Cancer* **15**, 722 (2015).

23. Locci, M., *et al.* Activin A programs the differentiation of human TFH cells. *Nat Immunol* **17**, 976-984 (2016).
24. Schmitt, N., *et al.* The cytokine TGF-beta co-opts signaling via STAT3-STAT4 to promote the differentiation of human TFH cells. *Nat Immunol* **15**, 856-865 (2014).
25. Epstein, M.A. & Barr, Y.M. Characteristics and Mode of Growth of Tissue Culture Strain (Eb1) of Human Lymphoblasts from Burkitt's Lymphoma. *J Natl Cancer Inst* **34**, 231-240 (1965).
26. EPKINLY [package insert]. Plainsboro, NJ: Genmab US, Inc. and North Chicago, IL: AbbVie Inc. 2023.
27. Laurent, C., Dietrich, S. & Tarte, K. Cell cross talk within the lymphoma tumor microenvironment: follicular lymphoma as a paradigm. *Blood* **143**, 1080-1090 (2024).
28. Ame-Thomas, P., *et al.* CD10 delineates a subset of human IL-4 producing follicular helper T cells involved in the survival of follicular lymphoma B cells. *Blood* **125**, 2381-2385 (2015).
29. Ame-Thomas, P., *et al.* Characterization of intratumoral follicular helper T cells in follicular lymphoma: role in the survival of malignant B cells. *Leukemia* **26**, 1053-1063 (2012).
30. Pangault, C., *et al.* Follicular lymphoma cell niche: identification of a preeminent IL-4-dependent T(FH)-B cell axis. *Leukemia* **24**, 2080-2089 (2010).
31. Richendollar, B.G., Pohlman, B., Elson, P. & Hsi, E.D. Follicular programmed death 1-positive lymphocytes in the tumor microenvironment are an independent prognostic factor in follicular lymphoma. *Hum Pathol* **42**, 552-557 (2011).

32. Falchi, L., *et al.* IBCL-460 Subcutaneous Epcoritamab With Rituximab + Lenalidomide (R2) in Patients With Relapsed or Refractory (R/R) Follicular Lymphoma (FL): Update from Phase 1/2 Trial. *Clin Lymphoma Myeloma Leuk* **22 Suppl 2**, S392 (2022).
33. Falchi, L., *et al.* ABCL-452 First-Line Treatment With Subcutaneous Epcoritamab + R-CHOP in Patients With High-Risk Diffuse Large B-Cell Lymphoma (DLBCL): Phase 1/2 Data Update. *Clin Lymphoma Myeloma Leuk* **22 Suppl 2**, S380 (2022).
34. Chan, A., Gao, Q. & Roshal, M. 19-color, 21-Antigen Single Tube for Efficient Evaluation of B- and T-cell Neoplasms. *Curr Protoc* **3**, e884 (2023).

METHODS

Patients: NCT #04663347 is a multi-arm phase 1/2 international trial of epcoritamab in combination with various standard-of-care therapies for patients with DLBCL or FL. Patients included in the present analysis included patients with DLBCL, who received epcoritamab in combination with either R-CHOP (newly diagnosed) or gemcitabine and oxaliplatin (relapsed/refractory), or FL, who received epcoritamab in combination with rituximab and lenalidomide (**Fig. 1a and Table 1**). Eligibility criteria, treatment schedule, and preliminary safety and efficacy results for each of these study arms were previously reported^{32,33}. As part of the study procedures, several patients underwent optional on-treatment biopsies during cycle 1 between days 22 and 28. Some subjects also underwent biopsy at the time of progression. Each patient provided written consent to participate in the study and had voluntarily opted into additional research biopsies. The study was assigned IRB Protocol #21-164, was approved as per 45 CFR 46.111 and/or 21 CFR 56.111 by the MSKCC Institutional Review Board/Privacy Board-A initially on April 5, 2021 and conducted in accordance with the principles outlined in the Declaration of Helsinki. Approval of the study with amendments was most recently issued on June 7, 2024.

Laboratory Analyses

Immunohistochemistry. Hematoxylin and eosin (H&E) stains were performed on 4- μ m formalin-fixed, paraffin-embedded tissue sections following routine processing. IHC studies were performed for diagnostic purposes, and, where sufficient tissue was available, additional IHC stains (**Supplementary Table 2**) were performed to study the

topographic distribution of various cell subsets in pretreatment, on-therapy, and relapse biopsies.

Multiparametric Flow Cytometry. Clinical flow cytometry was performed as previously described³⁴. Briefly, tissue was finely minced in RPMI 1640 growth medium using scalpel blades, then filtered, washed, and resuspended in RPMI. Following resuspension, cells were stained with an 21-antibody panel designed to assess for B- and T-cell subsets (**Supplementary Table 3**) and incubated at room temperature. Following staining and incubation, cells were lysed, fixed, washed, and resuspended. Up to 500,000 cells were acquired on a FACSymphony A3 flow cytometer (BD Biosciences). The results were analyzed with Woodlist software (Dr. B.L.Wood, University of Southern California).

Single-cell immune profiling. Single cell RNA FASTQ data was processed using Cellranger v6.0.2 *count* workflow to generate gene expression count matrices. TCR data was processed using Cellranger's *vdj* pipeline to generate cell-clonotype annotations. Processed RNA and ADT matrices were combined into a single Seurat v5.0.1 object (using the *CreateSeuratObject* function), into which TCR clonotype information was subsequently incorporated using *scRepertoire v1.7.2 combineExpression* function. Filtering was applied upon the merged data to only retain cells with (1) greater than 500 and less than 4000 detected unique RNA features, (2) less than 10000 total RNA molecules (3) less than 5 percent mitochondrial RNA reads and (4) less than 2500 total ADT molecules. RNA and ADT data were normalized

using Seurat's *NormalizeData* function with 'LogNormalize' and 'CLR' methods specified for each, respectively.

PCA was performed (using Seurat's *RunPCA* function) and to mitigate the effect of lane-specific and sample-specific covariates/batch effects, Harmony v1.0.0 *RunHarmony* function was used to correct embeddings. Elbow plots were manually inspected to determine the number of principal components to use downstream and a global UMAP was constructed using Seurat's weighted nearest-neighbor workflow upon corrected RNA and ADT data (n=14278). Using *clustree* v.0.5.0 produced tree diagrams for various resolution input values, cluster stability was evaluated to avoid over-clustering and optimize the number of communities selected. Subsequently, separate Seurat object for B and T-lymphocytes were produced by evaluation of and isolation by canonical marker expression. T-lymphocytes were further separated by first gating on CD3 and separating into CD8 and CD4 compartments using the ADT expression for each of those markers. The previously described UMAP construction and clustering steps were performed for each cell-subtype object. Specialized cell-types were labeled by manually evaluating differentially expressed genes and surface protein markers across clusters. Transcriptional and proteomic differences between treatment and clinical outcome groups were characterized using Seurat's implementation of the Wilcoxon-Rank Sum Test. Gene-set enrichment against hallmark, gene ontology, and canonical pathway terms was computed using the pre-ranked module in gseapy v1.0.6. RPKM-normalized read coverage tracks were generated using pyGenomeTracks v3.8.

***In vitro* killing assay.** CD8⁺ or CD4⁺ T-cells were isolated from healthy donor PBMCs using Dynabeads Untouched CD8⁺ or CD4⁺ T-cell Kits, respectively (Invitrogen). CD8⁺ and CD4⁺ T-cells were activated and differentiated for 5 days under the following conditions: all cells were stimulated with plate-bound anti-CD3 (clone OKT3, Biolegend, 5 µg/mL) and soluble CD28 (clone CD28.2, Biolegend, 1 µg/mL). The following cytokines were added to culture to drive differentiation into distinct T-cell subsets, as previously reported: Tc1 (IL-2, 50 IU/mL, IL-12, 5 ng/mL), Tfh (Activin A, 50 ng/mL, IL-12, 1 ng/mL, IL-23, 10 ng/mL, TGF-β, 1 ng/mL), Treg (IL-2, 50 IU/mL, TGF-β, 5 ng/mL, sodium butyrate, 100 µM). T-cells were then co-cultured with RAJI B-cells that had been stably transduced with luciferase (Lenti-LucOS, Addgene #22777) at a 10:1 T-cell:B-cell ratio. 24 hours later, cells were lysed and residual luciferase was measured using a Promega ONE-Glo EX Luciferase Assay System (#E6120). Viability was calculated by normalizing luciferin luminescence to RAJI cells cultured in the absence of T-cells.

Supplementary Figure 1. Expanded immunophenotyping of tumor biopsies from patients receiving epcoritamab-based therapy. (a) Immunohistochemistry of lymph node biopsies obtained from patient 10 at the timepoints indicated. (b) Flow cytometric quantification of CD20 expression on B-cells from patients with FL at the indicated timepoints. (c) Left, expression of surface CD20 as measured by single-cell antibody-derived tag abundance in patients achieving a CR versus PD as best response. Right, expression of *MS4A1* as measured by single-cell transcript abundance in patients achieving a CR versus PD as best response. (d) Single-cell transcriptomes from B-cells aligning to the *MS4A1* locus. *MS4A1* exons including 5' and 3' untranslated regions are shown. (e) Immunohistochemistry of lymph node biopsies obtained at the indicated timepoints from patients with DLBCL. P values determined by Mann Whitney test (c).

Supplementary Figure 2. Expanded single cell transcriptomic analysis of T- and B-cell phenotypes in patients receiving epcoritamab-based therapy. (a,b) Dot plot depicting average expression and frequency of expression of genes defining CD4⁺ (a) and CD8⁺ (b) T-cell subsets as indicated. (c,d) Differentially expressed genes between either CD4⁺ (c) or CD8⁺ (d) T-cells with (>1 cell with the same TCR CDR3 sequence) or without evidence of clonal expansion, stratified by best response. P value determined by Student's t-test, adjusted for multiple comparisons (c,d).

Supplementary Figure 3. Expanded functional analysis of T-cell subsets in patients receiving epcoritamab-based therapy. (c) Expression of Granzyme B, Tfh

markers (CXCR5, PD-1), and FoxP3 following T-cell activation and differentiation for 5 days *in vitro*.

Supplementary Table 1. Types of correlative analyses run on samples from NCT #04663347.

Patient N.	Pre-Tx		On-Tx			POD	
	IHC	FC	IHC	FC	scRNA	IHC	FC
1	yes	no	no	no	no		
2	yes	yes	no	no	no		
3	yes	no	yes	no	no		
4	yes	no	no	no	no		
5	yes	yes	yes	no	no		
6	yes	yes	yes	no	no		
7	yes	yes	yes	no	no		
8	yes	no	yes	yes	yes	yes	no
9	yes	yes	no	no	yes	yes	no
10	yes	no	yes	yes	yes		
11	yes	no	yes	yes	yes		
12	yes	yes	no	no	no		
13	yes	yes	yes	no	no		
14	yes	yes	no	no	no		
15	yes	yes	yes	no	yes		
16	yes	yes	yes	no	no	yes	yes
17	yes	no	yes	no	no		
18	yes	yes	yes	no	no		
19	yes	yes	no	no	yes		
20	yes	yes	yes	yes	yes		
21	yes	yes	yes	yes	no		
22	yes	yes	no	no	no		

Supplementary Table 2. Antibody clones used for immunohistochemistry analysis.

Antigen	Clone	Manufacturer
BCL2	124	Ventana
	PG-B6p	Dako
CD2	MRQ11	Cell Marque
CD3	LN10	Leica
CD4	SP35	Cell Marque

CD5	SP19	Ventana
	4C7	Leica
CD7	MRQ56	Cell Marque
	LP15	Leica
CD8	SP57	Ventana
	4B11	Leica
CD10	SP27	Ventana
	56C6	Leica
CD19	BT51E	Leica
CD20	L26	Dako
CD21	1F8	Dako
CD23	SP23	Ventana
	1B12	Leica
CD30	Ber-H2	Dako
CD79a	SP18	Ventana
	11E3	Leica
cMYC	Y69	Ventana
Cyclin D1	EPR2241	Abcam
	SP4	Thermo Scientific
EBER-ISH	N/A	Ventana
FOXP1	JC12	Abcam
Granzyme B	GrB7	Dako
HGAL	1H1-A7	Invitrogen
IGD	Polyclonal	Cell Marque
KI67-MIB1	MIB1	Dako
	30-9	Ventana
LMO2	1A9-1	Santa Cruz
MUM1	MUM1p	Dako
	EAU32	Leica
OCT2	MRQ-2	Cell Marque
P53	D07	Ventana
PAX5	SP34	Ventana
	1EW	Leica
SOX-11	MRQ58	Cell Marque
TDT	Polyclonal	Cell Marque
	SEN28	Leica
TIA1	2G9A10F5	Biogenex

Supplementary Table 3. Antibody clones used for flow cytometry analysis.

Antigen	Clone	Fluorochrome	Manufacturer	Catalog
---------	-------	--------------	--------------	---------

Kappa	Polytypic	FITC	Agilent	F043401-1
CD8	REA734	FITC	Miltenyi	130-110-815
Lambda	Polytypic	PE	Agilent	R043701-1
CD56	N901	PE	Beckman Coulter	IM2073U
CD25	BC96	PE-Dazzle594	BioLegend	302646
CD22	SJ10.1H11	PC5.5	Beckman Coulter	A80712
TCRCβ1	JOVI.1	BB700	BD Biosciences	7497974
CD19	J3-119	PC7	Beckman Coulter	IM3628U
CD10	ALB1	APC	Beckman Coulter	IM3633
CD7	8H8.1	APC-Alexa700	Beckman Coulter	A70201
CD45	2D1	APC-H7	BD Biosciences	641408
CD5	L17F12	BV421	Biolegend	364029
CD38	HIT2	BV480	BD Biosciences	566137
CD279	EH12.2H7	BV605	BioLegend	329924
CD20	2H7	BV650	BD Biosciences	563780
TCRγδ	11F2	BV711	BD Biosciences	624148
CD2	RPA-2.10	BV786	BD Biosciences	740960
CD26	M-A261	BUV395	BD Biosciences	744454
CD4	SK3	BUV563	BD Biosciences	612912
CD3	UCHT1	BUV737	BD Biosciences	612750
CD14	M5E2	BUV805	BD Biosciences	612903

Supplementary Table 4. Pathology review of FFPE specimens.

Disease	Patient ID	Best Response	Timepoint	CD20	PAX5	Other
FL	10	CR	On-Tx	Patchy membranous and cytoplasmic staining with variable downregulation (negative to dim to moderate intensity)	Strong nuclear	No other B cell markers
	15	CR	On-Tx	Negative	Strong nuclear	CD79a strong membranous staining
	16	CR	PD	Negative	Strong nuclear	No other B cell markers
	20	PD	On-Tx	Negative	Not performed	CD10 variable membranous staining
DLBCL	6	On-Tx	CR	Positive on necrotic cells	Not performed	
	7	On-Tx	CR	Positive on necrotic cells	Not performed	
	8	On-Tx	PR	Strong and diffusely membranous	Not performed	No other B cell markers
		POD	PR	Negative	Strong nuclear	No other B cell markers
	9	POD	PR	Negative	Strong nuclear	CD19 diffusely positive

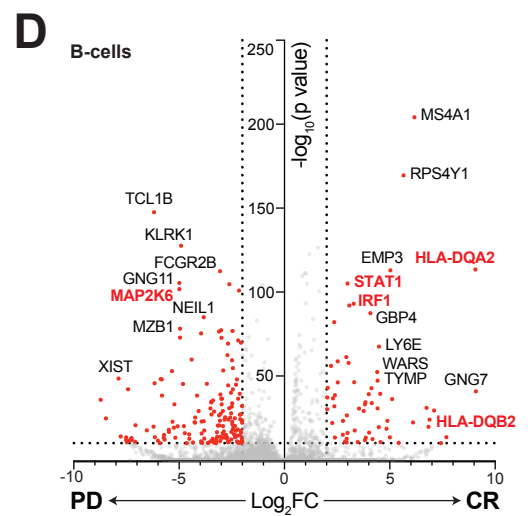
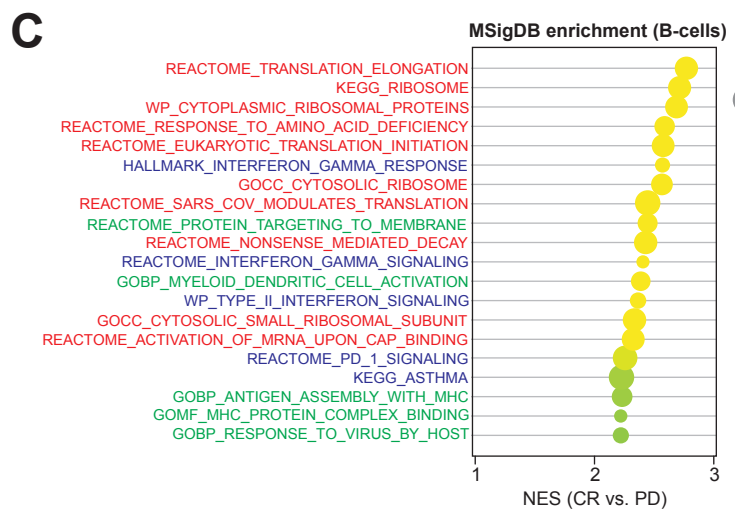
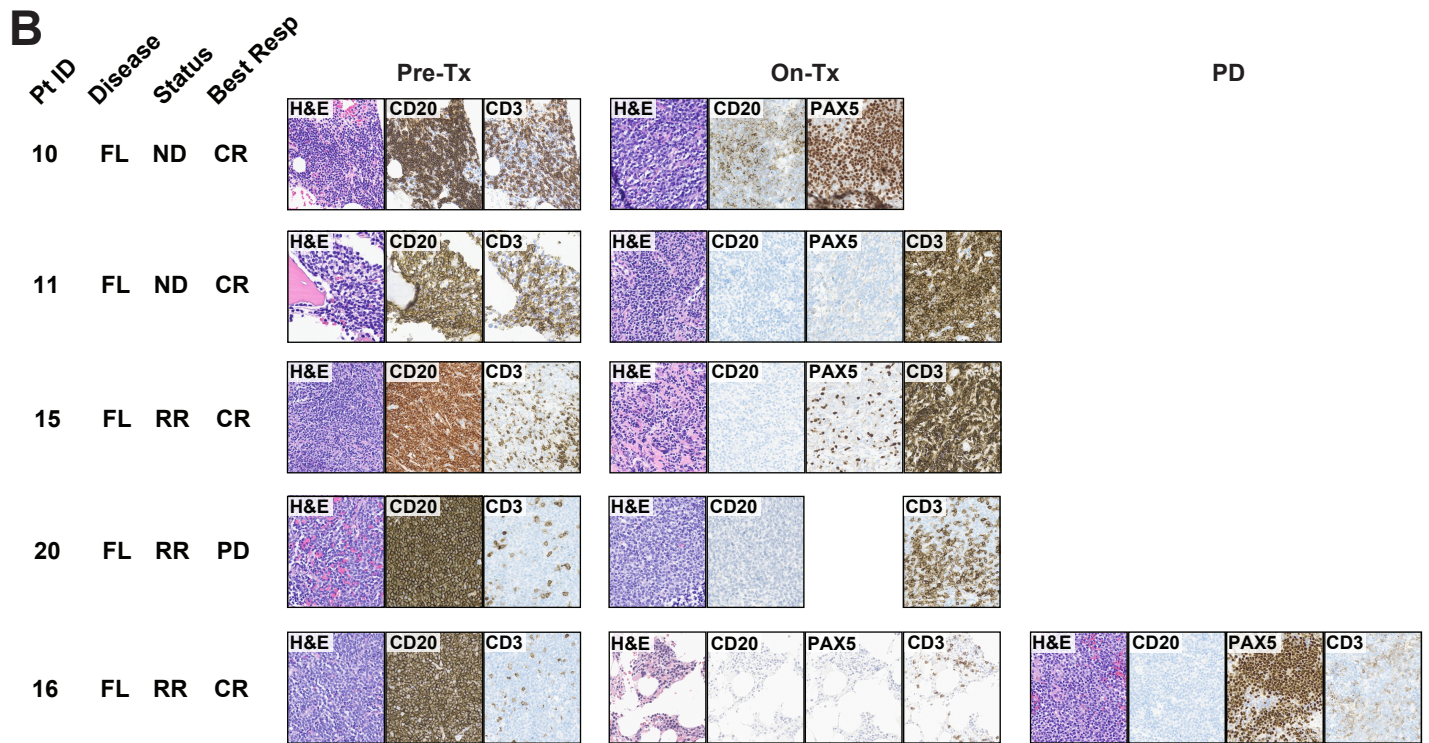
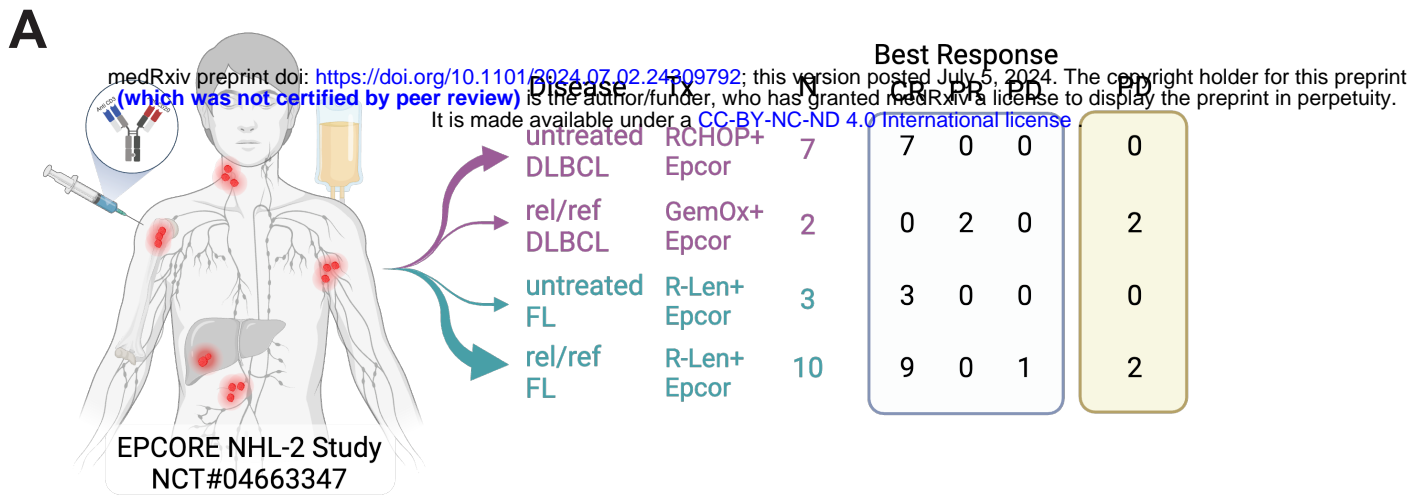


Figure 1.

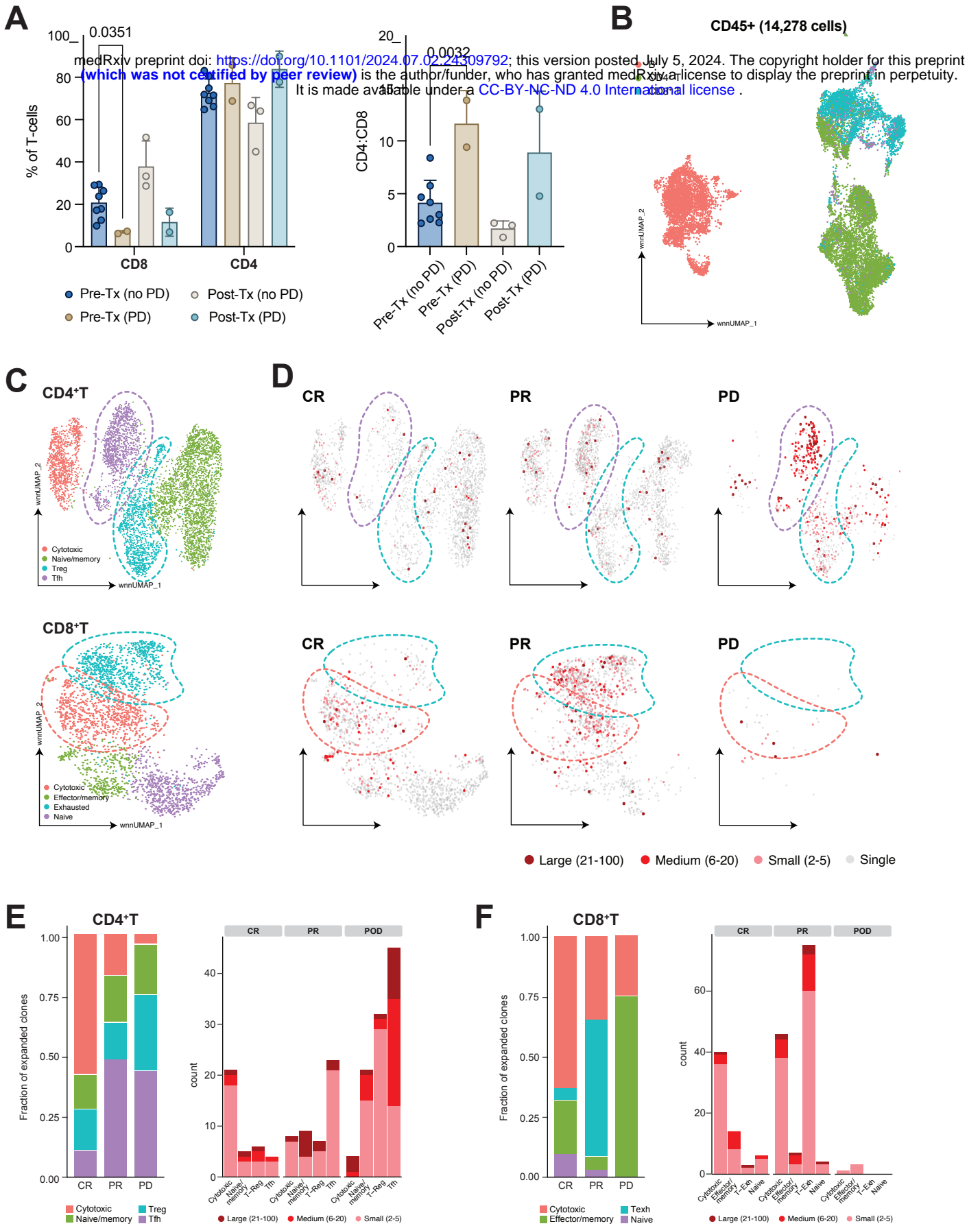
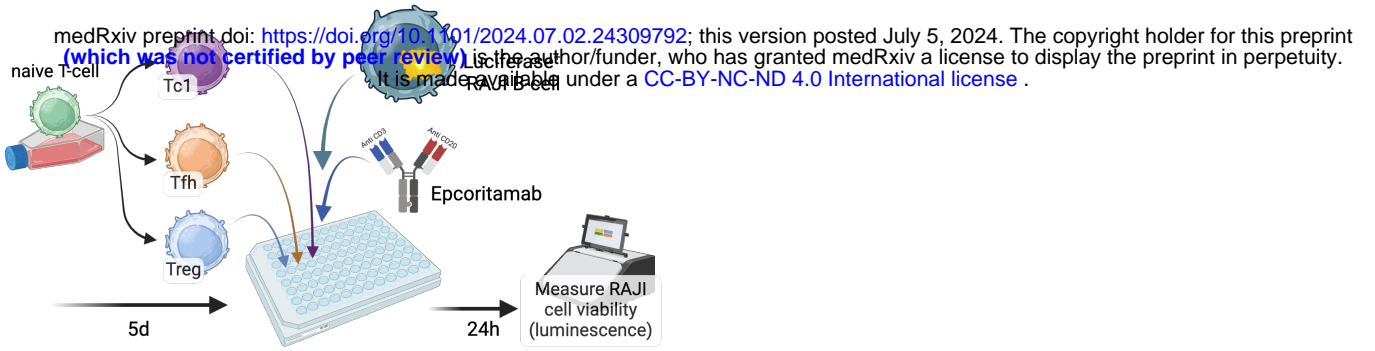
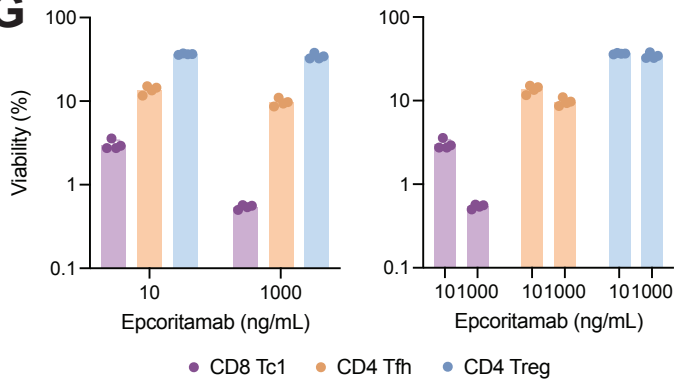


Figure 2.

F**G****Figure 3.**